Experiments on Natural Convection Heat Transfer in Low Aspect Ratio Enclosures

Y. Kamotani,* L. W. Wang,† and S. Ostrach‡
Case Western Reserve University, Cleveland, Ohio

Natural convection heat transfer in rectangular enclosures of aspect ratio less than and equal to 1 is investigated experimentally. The heat transfer and temperature fields were studied for various values of Rayleigh, aspect ratio, and Prandtl numbers. The experiments covered a range of Rayleigh numbers (Ra) between 10^4 and 4×10^7, aspect ratios (Ar) between 0.043 and 1.0, and Prandtl numbers (Pr) between 5.5 and 19,280 using water and various silicone oils. In case of $Ar=1.0$ the Nusselt number (Nu) was found to be nearly independent of Pr. For $Ar=0.2$, Nu was noticeably influenced by Pr in a certain range of Ra owing to the behavior of secondary cells. Nu for water in low aspect ratio enclosures was found to be proportional to $Ra^{0.3}$ in the boundary-layer regime, but there was an indication that Nu becomes eventually proportional to approximately $Ra^{0.25}$ at higher Ra as in case of $Ar=1.0$.

Nomenclature

Ar	= aspect ratio = H/L
g	= gravitational acceleration
H	= height of enclosure
k	= thermal conductivity of fluid
L	= length of enclosure
Nu	= Nusselt number = $Q/k\Delta TW$
Pr	= Prandtl number = ν/α
Q	= total heat input
Ra	= Rayleigh number = $g\beta(\Delta T)H^3/\nu\alpha$
T	= temperature of fluid
T_c	= cold wall temperature
T_h	= hot wall temperature
$T_b(x)$	= bottom wall temperature
$T_u(x)$	= upper wall temperature
W	= width of enclosure
(x,y)	= coordinate system defined in Fig. 1
α	= thermal diffusivity
β	= volumetric expansion coefficient
ΔT	= temperature difference = T_h-T_c
θ	= dimensionless temperature = $(T-T_c)/(T_h-T_c)$
θ_b	= $(T_b-T_c)/(T_h-T_c)$
θ_u	= $(T_u-T_c)/(T_h-T_c)$
ν	= kinematic viscosity

Introduction

In the existing work on natural convection in a rectangular enclosure with its vertical walls maintained at different temperatures, relatively little information is available on natural convection heat transfer in a low aspect ratio enclosure. According to the analysis by Cormack et al.,[1] in the limit as $Ar\to0$ the flow in the enclosure is driven by the buoyancy forces in the core region (the region away from the vertical walls) and the core flow is parallel. The heat transfer mechanism is mainly conduction, and the relatively weak convection in the horizontal direction is balanced by conduction in the vertical direction in the core. Bejan and Tien[2] analyzed the case of small but finite Ar and derived an expression for the Nusselt number for each of three characteristic flow regimes (the $Ra\to0$ regime, the intermediate regime, and the boundary-layer regime). They assumed the existence of parallel cores in all three regimes, which is not true under certain conditions, as shown by Ostrach et al.[3] In addition, several approximations were involved in deriving the Nusselt number expressions. Therefore the predictions by Bejan and Tien need experimental confirmations over wide ranges of the important parameters (Ra, Ar, and Pr).

At present there are only a few experimental studies available. Imberger[4] measured the values of Nu in the ranges $Ra=1.3\times10^6$-1.1×10^8 where $Ar=0.1$ and 0.019. Bejan et al.[5] covered the ranges $Ra=2.9\times10^8$-1.6×10^9 for $Ar=0.0625$. Both experiments used water. Sernas and Lee[6] measured heat transfer rates in air enclosures. In case of air, because of its relatively low thermal conductivity, heat loss from the surrounding walls is generally appreciable, and thus the thermal boundary conditions along the horizontal walls are less well-defined than in experiments with liquids. There are also a few numerical analyses (Cormack et al.,[7] Tseng,[8] and Lee and Sarnas[9]). Because a numerical analysis of natural convection in a low aspect ratio enclosure requires a long computation time the available numerical results covered limited ranges of the parameters.

The present work is intended to give a comprehensive picture on laminar natural convection heat transfer in two-dimensional low aspect ratio enclosures with thermally insulated horizontal walls by systematically varying the parameters Ra, Ar, and Pr. The experiment covers the ranges $Ra=10^4$-4.0×10^7, $Ar=0.043$-1.0, and $Pr=5.5$-19,280. The results are compared with the predictions by Bejan and Tien[2] and the available numerical and experimental results.

Experimental Apparatus and Procedure

A sketch of the present experimental setup is given in Fig. 1. The vertical walls of the container were made of 0.64-cm-thick copper plates. An electrical heating mat was bonded to the back of one of the copper plates, and the other plate was cooled by circulating water maintained at a constant temperature (±0.05°C) by a constant temperature bath. The horizontal walls were made of 0.64-cm-thick Plexiglas. Several container dimensions were used as listed in Table 1. In all cases the width of the containers was 25.4 cm. The whole

Presented as Paper 81-1066 at the AIAA 16th Thermophysics Conference, Palo Alto, Calif., June 23-25, 1981; submitted Jan. 4, 1982; revision received May 17, 1982.

*Associate Professor, Department of Mechanical and Aerospace Engineering. Member AIAA.

†Graduate Student, Department of Mechanical and Aerospace Engineering.

‡Professor, Department of Mechanical and Aerospace Engineering. Fellow AIAA.

Table 1 Container dimensions

H, cm	L, cm	A
7.62	7.62	1.0
2.54	12.70	0.20
2.54	20.32	0.125
2.54	40.64	0.0625
1.75	40.64	0.043

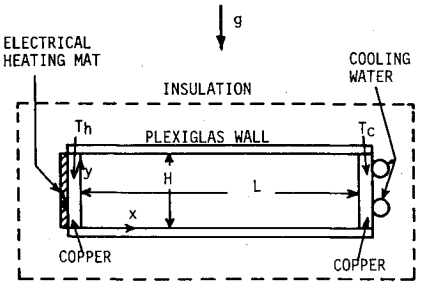

Fig. 1 Experimental setup.

setup was carefully wrapped around by 5-cm-thick fiberglas insulation to minimize the heat loss from the system to the surrounding. The test fluids were water ($Pr = 5.5$-7.1) and silicone oils SF96-100 ($Pr = 365$), SF96-350 ($Pr = 3375$), and SF96-2000 ($Pr = 19{,}280$). The various properties of the silicone oils were taken from Ref. 10.

The fluid properties were evaluated at the average temperatures of the hot and cold walls. To minimize the variations of the fluid properties (especially viscosity) within the container for a given run, the temperature difference $T_h - T_c$ was kept below 10°C throughout the experiment. Three thermocouples were imbedded in each of the hot and cold walls for wall temperature measurements. In addition several thermocouples were imbedded in the upper and bottom Plexiglas plates to measure temperature variations along the horizontal walls. A narrow slit (0.3 cm wide) was cut along the upper plate for temperature measurements inside the container by a thermocouple probe. The thermocouple outputs were read by a potentiometer. The slit was also used to inject dye from a hypodermic needle for qualitative flow visualization tests. The flow visualization tests revealed that the flow structures in all the containers used herein were very uniform in the spanwise direction except in relatively thin regions (of the order 5-10 mm) near the side walls.

Although the setup was carefully insulated, a certain amount of heat loss was expected from the horizontal walls and from the back of the heater. The heat loss from the system was estimated by comparing the electrical input to the heater with the amount of heat removed by the cooling water. The latter was calculated from the cooling water flow rate and the difference between the cooling jacket inlet and outlet temperatures measured by thermocouples. For this test the flow rate was adjusted so as to make the temperature difference large enough for the measurement but small compared to $T_h - T_c$. The heat loss measurements under various conditions showed that the heat loss increased slightly with decreasing $T_h - T_c$, but the loss remained within 7% of the total heat input over the ranges of the parameters studied herein. After the heat loss measurements, the cooling water flow rate was increased to make the cold wall temperature uniform, and the total electrical input to the heater was considered to be equal to the net amount of heat transferred from the hot wall to the cold wall.

The dimensionless heat transfer rate, Nusselt number was calculated from the relation

$$Nu = Q/k(\Delta T)W$$

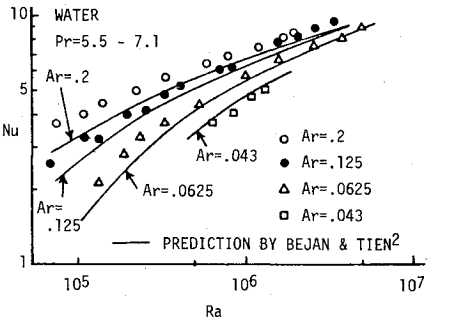

Fig. 2 Nusselt number in the intermediate regime.

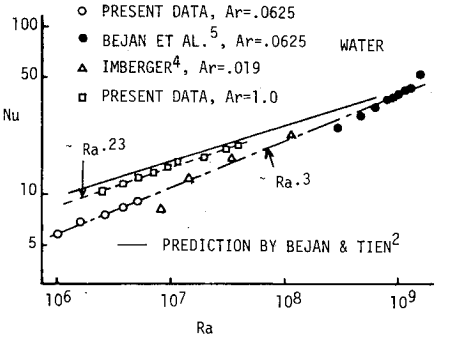

Fig. 3 Nusselt number in the boundary-layer regime.

The temperature difference $\Delta T = T_h - T_c$ was measured when the system was considered to be in a steady state judging from the wall temperature variations. Usually it took about 12 h to reach a steady state after the heater was turned on. The experimental error in the value of Nu was estimated to be ±10%.

Experimental Results

Heat Transfer Rate

The Nusselt number data for water ($Pr = 5.5$-7.1) for various values of Ar are presented in Fig. 2. Most of the data should fall within the intermediate regime according to the analysis by Bejan and Tien,[2] and their prediction of Nu for the regime is also shown in Fig. 2 for comparison. The data and the prediction agree well when Ar is less than about 0.1, but the model tends to underpredict when Ar is larger than 0.2. Bejan and Tien assumed a simple unicellular flow pattern in the intermediate regime for the integral method they used, but, according to the flow pattern observations made in the present study and those by Ostrach et al.,[3] the flow structure becomes very complex when Ar is larger than about 0.2. Secondary cells appear in the end regions (the regions near the vertical walls), and the core flow is no longer parallel. The data and prediction show that as Ra increases, the values of Nu for various Ar tend to collapse to one curve; that is, Nu becomes a function of Ra only, which is a characteristic of the boundary-layer regime.

Some of the data in Fig. 2 at high Ra in fact belong to the boundary-layer regime according to the classification by Bejan and Tien.[2] All the data taken by Bejan et al.[5] and some of the data by Imberger[4] also belong to this regime. They are plotted in Fig. 3. Also shown in the figure are the values of Nu for $Ar = 1.0$ measured in the present experiment with water. A statistical analysis based on the data by Bejan et al. and the present data for the same aspect ratio showed that Nu is proportional to $Ra^{0.3}$ above $Ra = 5 \times 10^5$ as indicated in Fig. 3. The data taken by Imberger for $Ar = 0.019$ and those for $Ar = 0.125$ in Fig. 2 have almost the same power of Ra beyond $Ra = 1.5 \times 10^7$ and 2×10^5, respectively. In case of $Ar = 1.0$ Nu was found to be proportional to $Ra^{0.23}$ as seen in Fig. 3.

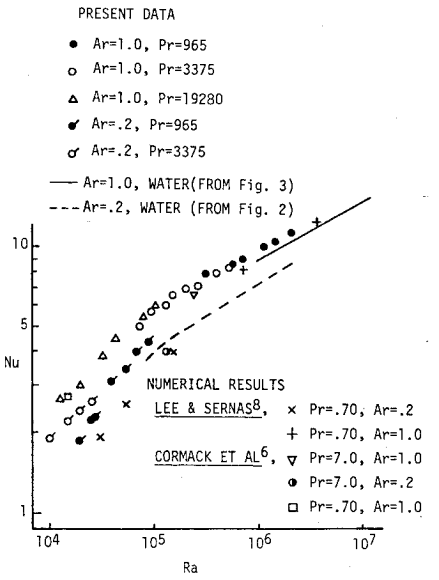

Fig. 4 Effect of *Pr* on *Nu*.

The data for $Ar=0.2$ in Fig. 2 were found to follow $Ra^{0.24}$ above $Ra=1.5\times10^5$. Therefore it seems that when Ar is less than about 0.1, Nu become proportional to $Ra^{0.3}$ beyond a certain value of Ra, and when Ar is above about 0.1, the power of Ra decreases slightly, with increasing Ar becoming equal to 0.23 for $Ar=1.0$. Bejan and Tien predicted in the boundary-layer regime that

$$Nu=0.623Ra^{0.2}$$

The present data for $Ar=1.0$ follow closely the prediction as seen in Fig. 3, but it overpredicts Nu when Ar is small.

The trend of the data in Figs. 2 and 3 indicates that all the data, including those for $Ar=1.0$, converge eventually at high Ra (about $Ra=10^9$), and Nu becomes independent of Ar. At high Ra it is expected that heat transfer is predominantly determined by the boundary-layer type flows along the hot and cold walls. Since it is known that in case of natural convection heat transfer in the boundary layer along a vertical flat plate, Nu is proportional to $Ra^{0.25}$, it is reasonable to expect that Nu for rectangular enclosures possesses nearly the same proportionality as $Ra\to\infty$. The data for $Ar=1.0$ in Fig. 3 already follow ¼ power of Ra within the experimental errors. Then the aforementioned prediction by Bejan and Tien seems to be reasonable, if it is applied in such $Ra\to\infty$ regime.

The effect of Pr on Nu was studied using silicone oils of various viscosity values for $Ar=1.0$ and 0.2. The results are presented in Fig. 4. Since a wide range of viscosity was studied, the ranges of Ra covered by the fluids did not necessarily overlap. Figure 4 also shows some of the available numerical results of Nu for air and water.

In case of $Ar=1.0$, all the silicone oil data ($Pr=965$-19,280) seem to follow almost the same trend within the experimental errors. However, there is a small but noticeable difference between the silicone oil data with $Pr=965$ and the water data with $Pr=5.5$-7.1. Nu seems to increase very slightly with Pr, which is consistent with the result of the numerical analysis by De Vahl Davis[11] for $Ar=1.0$. The numerical results given in Fig. 4 are in good agreement with the present experimental data.

In the case of $Ar=0.2$ the data are more scattered among various Pr, especially when $Ra<10^5$. Including the numerical results for air, Nu can be seen in Fig. 4 to increase consistently with Pr. According to the present dye trace experiment, cellular fluid motions were noticeable in the end regions, especially when Pr was large. The appearance of secondary

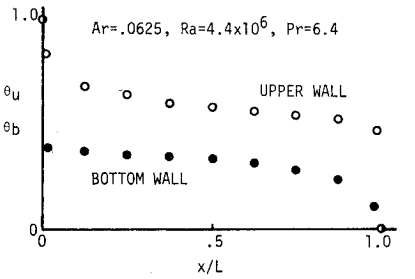

Fig. 5 Temperature distributions along horizontal walls.

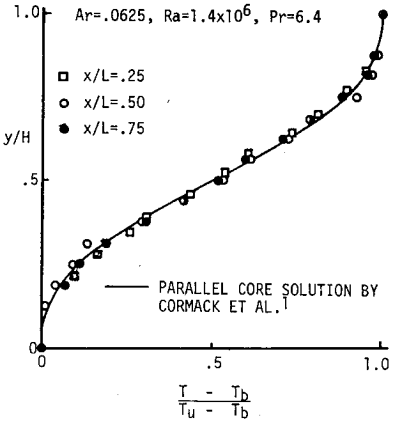

Fig. 6 Temperature distributions in the core regions.

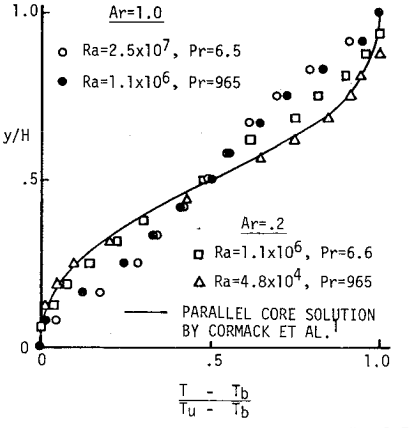

Fig. 7 Temperature distributions at $x/L=0.5$.

cells in low aspect ratio enclosures has been recently reported by Simpkins and Dudderar.[12] From their visualization studies they determined the onset condition for the appearance of secondary cells as

$$RaAr^{¼}\sim6.4\times10^5$$

However, our experimental observations covering a wider range of Pr indicated dependence of the onset condition on Pr as well as Ra and Ar. To clarify this matter we are currently studying the onset condition experimentally and analytically. The secondary cells caused substantial changes in the end region temperature distributions as shown below. With the appearance of secondary cells, the whole flow structure also changes drastically (Ostrach et al.[3]). Although it is not immediately apparent whether Nu increases or decreases with the appearance of cells, the present data showed an increase of Nu in the ranges of the parameters studied herein.

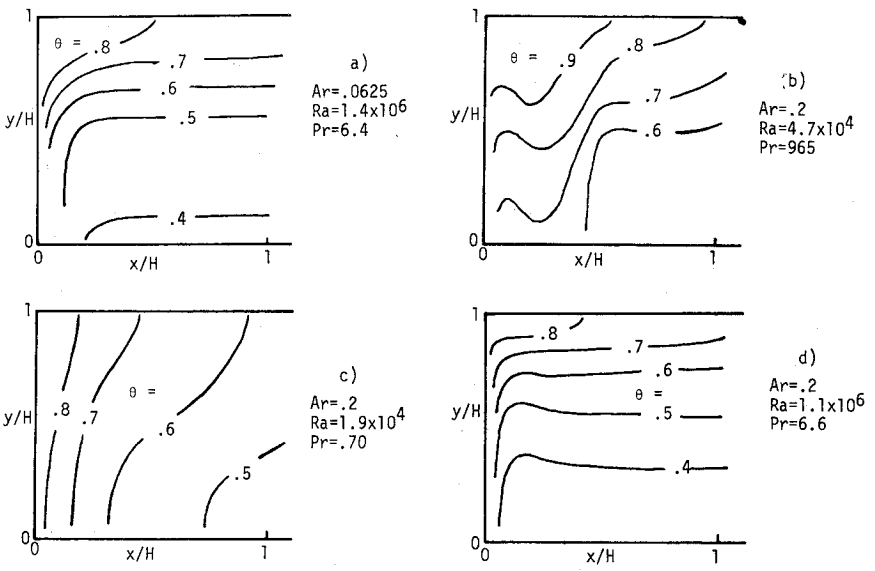

Fig. 8 Isotherms near hot wall for $Ar = 0.0625$

Temperature Distribution

Figure 5 shows the temperature distribution along the bottom and top walls for water and $Ar = 0.0625$. Except in the regions very close to the hot and cold walls, the temperature variations in the x direction are relatively small. This means that in the core region the convection of heat in the x direction is much larger than the heat transfer in the y direction so that the length of the core region has relatively small influence on the overall heat transfer rate as seen in the aforementioned Nu behavior in the boundary-layer regime.

Figure 6 shows the temperature distributions in the y direction at three x locations for water and $Ar = 0.0625$. All the profiles are similar and agree with the parallel core solution given by Cormack et al.,[1] which suggests that the flow in the core region is parallel. The temperature distributions in the midplane for various values of Ar and Pr are given in Fig. 7. When $Ar = 0.2$, $Ra = 4.8 \times 10^4$, and $Pr = 965$, the temperature distribution at the midplane has the parallel core profile despite the facts that the secondary cells are present in the end regions and the core flow is not really parallel as described in the work by Ostrach et al.[3] When $Ar = 0.2$, $Ra = 1.1 \times 10^6$, and $Pr = 6.6$, the temperature profile deviates from the parallel core solution, especially along the top wall. When conducting the experiments with water, owing to the viscosity variation with temperature, the fluid motion in the hot region was found to be slightly more active than that in the cold region. This is a part of the reason for the deviation of the temperature profile from the parallel core solution. But the deviation also shows that as the convection of heat in the x direction becomes large, the hot and cold fluids concentrate more along the top and bottom walls, respectively; namely, the thermal boundary layers appear along the horizontal walls. Such flow behavior is evident for $Ar = 1.0$ over a wide range of Pr as shown in Fig. 7.

Some typical isotherm patterns near the hot wall or in the whole container for various values of Ar are presented in Figs. 8 and 9. In case of $Ar = 0.0625$, $Ra = 1.4 \times 10^6$, and $Pr = 6.4$ (Fig. 8a), the fluid outside the thermal boundary layer is stably stratified, and no noticeable secondary cells were present in the end regions. When $Ar = 0.2$, $Ra = 4.7 \times 10^4$, and $Pr = 965$ (Fig. 8b), the isotherms are very much distorted owing to the presence of a secondary fluid motion with clockwise rotation outside the boundary layer along the hot wall. At comparable Ra but with air (Fig. 8c) the isotherm pattern is much less distorted, which implies no or very weak secondary cells in case of air. The difference in the isotherm patterns between the above two cases is reflected in the difference in Nu as discussed above. No Nu data were taken for air in the present experiment, because the heat loss from the

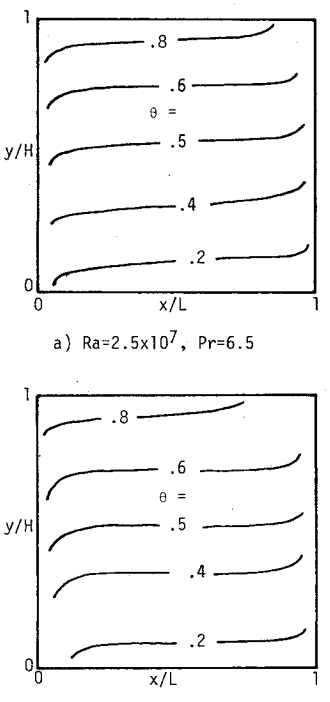

Fig. 9 Isotherm patterns for $Ar = 1.0$.

system was expected to be larger than that for the liquid tests. The secondary cells were also observed at $Ar = 0.2$, $Ra = 1.1 \times 10^6$, and $Pr = 6.6$ (Fig. 8d), but as the figure indicates, the isotherm pattern is not distorted substantially. The above observations indicate that the influence of the secondary cells on the temperature distributions is a complex function of Pr, Ra, and Ar. Figure 9 shows that in case of $Ar = 1.0$, the general isotherm patterns do not change significantly over a wide range of Pr, which is consistent with the fact that Nu changes very slightly with Pr. The secondary cells were observed under the conditions given in Fig. 9.

Summary of Results

Experiments were carried out to investigate natural convection heat transfer in rectangular enclosures of aspect ratio less than and equal to 1. The heat transfer rate and temperature field were studied over wide ranges of the parameters

Ra, Pr, and *Ar*. The results of the present experiments indicate the following:

1) The *Nu* prediction by Bejan and Tien[2] in the intermediate regime agrees well with the present data for water when *Ar* is less than about 0.1, but the flow structure becomes more complex than assumed in the model at larger *Ar*.

2) When $Ar=0.2$, the heat transfer rate is found to depend strongly on *Pr* because of the effect of *Pr* on secondary cells.

3) In the boundary-layer regime, *Nu* is proportional to $Ra^{0.3}$ when *Ar* is less than about 0.1; and when *Ar* is above 0.1, the power of *Ra* decreases slightly with increasing *Ar*.

4) There seems to be an $Ra\to\infty$ regime in which *Nu* is proportional to $Ra^{0.25}$, as in case of natural convection along a vertical flat plate.

Acknowledgment

The present work was supported by the U.S. Air Force Office of Scientific Research under Grant F49620-79-C-0033.

References

[1]Cormack, D. E., Leal, L. G., and Imberger, J., "Natural Convection in a Shallow Cavity with Differentially Heated End Walls. Part 1. Asymptotic Theory," *Journal of Fluid Mechanics*, Vol. 65, Pt. 2, 1974, pp. 209-229.

[2]Bejan, A. and Tien, C. L., "Laminar Natural Convection Heat Transfer in a Horizontal Cavity with Different End Temperatures," *Journal of Heat Transfer*, Vol. 100, No. 4, 1978, pp. 641-647.

[3]Ostrach, S., Loka, R. R., and Kumar, A., "Natural Convection in Low Aspect Ratio Rectangular Enclosures," in *Natural Convection in Enclosures*, edited by K. E. Torrance and I. Catton., Heat Transfer Division of ASME, HTD-Vol. 8, 1980, pp. 1-10.

[4]Imberger, J., "Natural Convection in a Shallow Cavity with Differentially Heated End Walls. Part 3. Experimental Results," *Journal of Fluid Mechanics*, Vol. 65, Pt. 2, 1974, pp. 247-260.

[5]Bejan, A., Al-Homond, A. A., and Imberger, J., "Experimental Study of High-Rayleigh Number Convection in a Horizontal Cavity with Different End Temperatures," *Journal of Fluid Mechanics*, Vol. 109, Aug. 1981, pp. 283-299.

[6]Sernas, V. and Lee, E. I., "Heat Transfer in Air Enclosures of Aspect Ratio Less Than One," *Journal of Heat Transfer*, Vol. 103, No. 4, 1981, pp. 617-622.

[7]Cormack, D. E., Leal, G. G., and Sienfeld, J. G., "Natural Convection in a Shallow Cavity with Differentially Heated End Walls. Part 2. Numerical Solution," *Journal of Fluid Mechanics*, Vol. 65, Pt. 2, 1974, pp. 231-246.

[8]Tseng, W. F., "Numerical Experiments on Free Convection in a Tilted Rectangular Enclosure of Aspect Ratio 0.5," Clarkson College, Potsdam, N.Y., Rept. MIE-050, 1979.

[9]Lee, E. I. and Sernas, V., "Numerical Study of Heat Transfer in Rectangular Air Enclosures of Aspect Ratio Less than One," ASME Paper 80-WA/HT-43, 1980.

[10]*Silicone Fluids Technical Data Book S-9B*, Silicone Products Department, General Electric Company, Waterford, N.Y., 1964.

[11]Davis, De Vahl, "Laminar Natural Convection in an Enclosed Rectangular Cavity," *International Journal of Heat and Mass Transfer*, Vol. 11, 1968, pp. 1675-1693.

[12]Simpkins, P. G. and Dudderar, T. D., "Convection in Rectangular Cavities with Differentially Heated End Walls," *Journal of Fluid Mechanics*, Vol. 110, Sept. 1981, pp. 433-456.